**Research Article**

Ravi Gugulothu*, Narsimhulu Sanke, Naga Sarada Somanchi, Vikas Normalla, Farhana Akter and Banoth Dhola Ykuntam Sunil

# A numerical study of water based nanofluids in shell and tube heat exchanger

https://doi.org/10.1515/ehs-2022-0155
Received November 23, 2022; accepted January 14, 2023; published online March 17, 2023

**Abstract:** This numerical investigation is made to estimate the effect of $Al_2O_3$ and Cu nanofluids on heat transfer rate, friction factor and thermal performance factor of a shell and tube heat exchanger. Mass flow rates of shell side (water) fluid are varied. Water based nanofluids are used inside the tubes with 0.01, 0.03, and 0.05% volume concentrations of $Al_2O_3$ and Cu nanofluids. Nusselt number obtained from the present investigation is compared with Dittus–Bolter equation and Pongjet Pomvonge et al. and found to be in good agreement with a maximum deviation of 3%. The Nusselt number of the dispersed nanofluids increased with the increase of nanofluids volume concentrations and shell side mass flow rate. In this study, maximum enhancement in Nusselt number is 7.50%, 8.65%, and 9.61% for $Al_2O_3$, and 1.46%, 2.23%, and 3.18% for Cu nanofluid respectively at 0.01, 0.03, and 0.05% volume concentrations were compared to base fluid as water. Friction factor is highest by 58.00% at 0.05% volume concentration of $Cu/H_2O$ nanofluid when relate to $Al_2O_3/H_2O$ nanofluid. Thermal Enhancement factor achieved is highest for $Al_2O_3/H_2O$ nanofluid.

**Keywords:** friction factor; heat exchangers; heat transfer techniques; nanofluids; thermal performance factor.

***Corresponding author: Ravi Gugulothu**, Department of Mechanical Engineering, JNTUH College of Engineering Hyderabad, Hyderabad, Telangana, India, E-mail: ravi.gugulothu@gmail.com
**Narsimhulu Sanke, Naga Sarada Somanchi and Vikas Normalla,** Department of Mechanical Engineering, JNTUH College of Engineering Hyderabad, Hyderabad, Telangana, India, E-mail: nsanke@osmania.ac.in (N. Sanke), nagasaradaso@gmail.com (N.S. Somanchi), vikas35.narmala@gmail.com (V. Normalla)
**Farhana Akter,** Department of Physics, National University of Bangladesh, Bangladesh, India, E-mail: farhanabithi309@gmail.com
**Banoth Dhola Ykuntam Sunil,** Department of Mechanical Engineering, Institute of Aeronautical Engineering, Hyderabad, Telangana, India, E-mail: sunilbdy@gmail.com

## 1 Introduction

Energy and water are the two major things in this modern century to develop any country (Gugulothu et al. 2017a), each and every country facing a problem with huge scarcity of the above two things (Somanchi et al. 2015a). Due to tremendous growing of population and industries, demand of energy is growing more and more to supply sufficient energy to the world energy hunger only option is conservation of energy (Thakur et al. 2021). A Heat exchanger (HE) is an apparatus that can transfer heat from hot to cold fluids between two or more fluids (Gugulothu et al. 2022a; Reddy et al. 2017). Many industries are using shell and tube heat exchangers (STHX) in engineering practice to exchange heat for heating and cooling processes, due to reliability, versatility, technological up-gradation, ease of manufacturing, and operating at a higher pressure and temperature (Ahmed et al. 2021c). Beyond this STHX are the most popular equipment in oil, food, and chemical processing industries which can help to save and produce energy from the waste in the form of reheat (Gugulothu et al. 2021; Somanchi et al. 2014a; Somanchi et al. 2015b). For design engineers and utilizers, it is a prime motto to design optimum STHX by considering design parameters (Gugulothu et al. 2022b). Baffles are playing a key role to enhance heat transfer rate, i.e. segmental, helical, and ladder-type baffles induce cross-fluid flow over the tubes to improve their performance of it. Among these heat exchangers, helical-shaped heat exchanger offers more advantages like service life, fewer vibrations, and heat transfer coefficient (HTC) (Reddy et al. 2017).

According to Ahmed et al. (2022) industries are facing problems improving thermal performance which can boost the energy systematic methods to augment the heat transfer rate by reducing the installation price and maintenance of the industry. Gugulothu et al. (2019) numerically studied the 40° helical baffles STHX based on TEMA standards, further continued by Gugulothu et al. (2022b) designed 40° helical baffles STHX based on TEMA standards using RSM methods. Gugulothu et al. (2017b) and Somanchi et al. (2014b) listed three different methods to enhance heat transfer rate active,

passive, and compound techniques to minimize heat exchanger area, and to improve energy generation and fuel efficiency. The difference, advantages, and disadvantages between active and passive techniques are listed/given by Niwalkar et al. (2019). The passive method is an attractive one for research, among the heat transfer enhancement techniques (Gugulothu et al. 2017c; Sarada et al. 2014).

Common heat transfer (HT) aqueous, such as oil, propylene, ethylene glycol, and water are utmost popular fluids for industries (Gupta et al. 2014; Said et al. 2014; Reddy et al. 2015). The heat transfer rate is lesser, adequate to the poor thermal conductivity of conventional fluids. Many researchers have reported that to move towards a new engineering fluid which is nano (<100 nm) in size called nanofluids, due to greater potential for HT enhancements by being suspended in base fluid (Gugulothu et al. 2017d; Shilpi and Aggarwal 2020; Sundar et al. 2013). Nanofluids become attractive to innumerable researchers since they are observed to enhance numerous physical and chemical properties like thermal conductivity, diffusivity, viscosity, and stronger and more attested thermal performances than regular fluids due to the occurrence of suspended nanoparticles (Shilpi and Aggarwal 2020). These advantages make nanofluids promising heat transfer fluids to be used for heat transfer enhancement (Fares et al. 2020). Zeinali et al. (2007) noticed that adding nanoparticles to base fluid generates considerable enhancement of HT. Thakur et al. (2020) listed nanospheres uniformly dispersed when compared to the nanocapsules.

Ahmed et al. (2021b) numerically explore the entropy generation, thermal-hydraulic, and turbulence characteristics of a nuclear rod in a triangular rod array using $TiO_2$, $Al_2O_3$, and Graphene Oxide water-based nanofluids at various volume concentrations. They found that the entropy decreases, and increases kinetic energy with an enhancement in the volume fraction of nanofluids. They concluded that $TiO_2$ has the highest entropy, then $Al_2O_3$ is the second highest and Graphene Oxide has the truncated entropy generation among the studied nanofluids. Ahmed et al. (2021a) numerically explore the thermohydraulic performance of $TiO_2$, $Al_2O_3$, and Graphene Oxide/water as a coolant by using 1%, 2%, and 4% volume fractions of nanofluids to evaluate both global and local parameters. They found that the $Al_2O_3$ nanofluids at 4% volume fraction show the potential candidates. Zeinali-Heris et al. (2012) numerically investigated HT in a square cross-section duct using CuO, $Al_2O_3$, and Cu nanofluids. They noticed that the Nusselt number is enhanced by increasing volume concentration and decreasing the size of nanoparticles, the enhancement in Nusselt number is up to 77% for Cu, 68% for CuO, and 59% for $Al_2O_3$ nanofluids at 4% volume concentrations of 10 nm nanoparticles.

Niwalkar et al. (2019) experimentally explore the enhancement of HT coefficient in a shell and helically coiled tube HE utilizing $SiO_2$/water nanofluids by varying volume concentrations differing from 0.05 to 0.25% with different hot fluid flow rates, were cold fluid flow rate is constant. They found that the HTC of $SiO_2$/water nanofluids was 28.71% elevated than the base fluid, 52.61% elevated friction factor, and 62.60% elevated pressure drop compared to the base fluid. Gugulothu and Sanke (2022a) numerically studied STHX with 22% cut baffles (segmental) using $Al_2O_3$, CuO, and $SiO_2$ nanofluids by varying 1, 3, and 5% volume concentrations. Further, Gugulothu and Sanke (2022b) continued with the same nanofluids using segmental (22% Cut baffles), and helical baffles (HB) (20°, 30°, and 40°). They noticed that 40° HB proved higher HT and $Al_2O_3$ is shown best nanofluid among the studied nanofluids. Kaleru et al. (2022a) theoretically and numerically studied the STHX with $Al_2O_3$, Graphene Oxide, $TiO_2$, single wall carbon nanotube, and MXene water-based nanofluids for 1, 3, and 5% volume concentration. They found that graphene oxide provided the highest HTC among the studied nanofluids.

Maghrabie et al. (2021) experimentally studied the effects of the inclination angle (0°, 30°, 60°, and 90°) of a shell and helically coiled tube HE utilizing $SiO_2$/water, and $Al_2O_3$/water nanofluids by varying 0.1%, 0.2%, and 0.3% volume flow. They found 11%, 8.3%, and 7.5% enhancement in coil Nusselt number for water, $SiO_2$/water, and $Al_2O_3$/water nanofluids with 0.1% volume flow. Heris et al. (2011) numerically explored the convective HT in a triangular duct using $Al_2O_3$/water nanofluids parameters effects like diameters, and volume concentrations. They concluded that the Nusselt number the increases with the increase of volume concentrations and decrease of nanoparticle diameter. Velagapudi et al. (2008) experimentally explore the thermophysical characteristics of $Al_2O_3$, Cu, CuO, $TiO_2$, etc. nanofluids for various base fluids like engine oil, ethylene glycol, and water. From their study, they developed new correlations and compared them with existing literature models. Pak and Cho (2007) experimentally investigated HT and friction behaviors of dispersed fluids in turbulent fluid flow regimes through the circular pipe, and suggested higher thermal conductivity and larger size nanoparticles are good for better HT.

Malika and Sonawane (2021) investigated the efficiency of a 3D artificial illuminated sono photocatalytic reactor using hybrid nanofluid to remove toxic fragments from industrial waste, using response surface methodology (RSM) and artificial neural network (ANN) method. They found that the reactor time is less than 60 min for 0.5% vol. nanofluid concentration at 60 °C nanofluid temperature. Kanti et al. (2021a) numerically investigated the heat transfer and fluid

flow characteristics of fly ash water based nanofluid ranging from 0.1 to 1.5% vol. concentration under constant heat flux. They found that 9.4%, 36% friction factor and the Nusselt number respectively at 1.5% vol. concentration when compared with base fluid. Kanti et al. (2021b) experimentally studied the heat transfer coefficient and friction factor for the flow of fly ash nanofluid ranging from 0.5 to 2.0% vol. under constant heat flux at 30 °C of fluid temperature. They found that the 1.21, 1.18, and 1.42 are the highest thermal conductivity ratio, viscosity ratio, and maximum performance evaluation criteria respectively for a 2% vol. concentration at 30 °C when compared to the base fluid.

Kanti et al. (2021c) experimentally evaluated the heat transfer coefficient and friction factor using fly ash and fly ash-Cu hybrid nanofluid ranging from 0.5 to 2.0% vol. concentrations under constant heat flux by varying 30–60 °C of temperature. They found that the viscosity, thermal conductivity, and the heat transfer rate of hybrid nanofluid are higher than the base fluid (water), and fly ash nanofluid. The maximum Nusselt number augmentation is 15.6%, 93.5% for fly ash-Cu hybrid nanofluid, fly ash nanofluid when compared with base fluid, and 1.65, 1.87 are the maximum thermal performance factor for fly ash and hybrid nanofluid respectively at 2% vol. at inlet temperature of 60 °C. Kanti et al. (2021d) numerically and experimentally studied fluid flow and heat transfer characteristics of fly ash-Cu/water hybrid nanofluid ranging from 0.5 to 2.0% vol. at a 30 °C of fluid inlet temperature under constant heat flux. They found that the 57.1%, 8.95% are the maximum augmentation in Nusselt number for fly ash-Cu hybrid nanofluid, fly ash nanofluid respectively at a 2.0% volume concentrations, higher pressure drop in case of hybrid nanofluid were compared with fly ash and water. They noticed 1.52 is the maximum thermal performance factor value at 2.0% vol. concentrations.

Malika et al. (2021) numerically and experimentally investigated the heat transfer performance in STHX using 0.01% vol. concentration of CuO–ZnO/water hybrid nanofluid under turbulent fluid flow condition. They found that 13%, 33%, and 7% enhancement in pressure drop, the Nusselt number, and thermal efficiency respectively. They noticed 1.45 is the maximum thermal performance factor. Malika and Sonawane (2022) used $Fe_2O_3$–$TiO_2$/water hybrid nanofluids ranging from 1 to 2% vol. concentration in the presence of RSM tool to improve the photocatalytic degradation. Nowadays computational fluid dynamics (CFD) simulations are accomplish to avoid the greater cost on experimental works; most of the literature investigations are accomplish numerical simulations on single phase nanofluids and found good results by considering nanofluids are homogenous fluids (Mashayekhi et al. 2017). Numerous researchers evaluated the HT characteristics of nanofluids in different heat exchangers numerically as well as experimentally. Similar studies on inclined helical baffles STHX are scarce. Hence, in the present work, numerical investigations are carried out with inclined helical baffle heat exchanger using $Al_2O_3$ and Cu nanofluids with water as base fluid.

## 2 Geometry

Figure 1 is showing the assembly of STHX with segmental and helical baffles, Figure 2 is indicating 40° helical baffles with 832 mm length, and 31.75 mm tube pitch which is used in this study. Figure 3 shows the meshed geometry of 40° helical baffles STHX described in literature Gugulothu and Sanke (2022a), which contains outlet and inlet of cold, hot fluid inlet and outlet valves, four numbers of tubes with 25.40 mm of outer diameters to carry the cold fluid as well as nanofluids inside the tubes which is calculated using Equation (1).

## 3 Governing equation and boundary conditions

Governing equation and boundary conditions are given in literature Gugulothu and Sanke (2022a), Gugulothu and Sanke (2022b), Kaleru et al. (2022a), and Kaleru et al. (2022b). In this research paper author used $Al_2O_3/H_2O$, and $Cu/H_2O$ nanofluids ranging from 1 to 5% volume concentrations which are passing through tubes at constant mass flow rate as 0.22 kg/s, and hot water is travelling in shell side ranging from 0.23 to 0.43 kg/s. The fluid properties are given in Table 1 which is calculated using equations in literature Kaleru et al. (2022a) for base fluid, and Equations (7)–(10) for nanofluids at 343.15 K for hot fluid and 301.15 K for cold fluid temperatures. Grid independent test is done in previous research paper which is cited in literature Gugulothu and Sanke (2022b).

## 4 Data reduction

Tube inner diameter is (Kaleru et al. 2022a):

$$d_i = 0.8 \times d_0 \tag{1}$$

Friction factor is (Mohammadiun et al. 2016)

$$f_t = \frac{2\Delta P}{\rho v^2}\frac{d_i}{L} \tag{2}$$

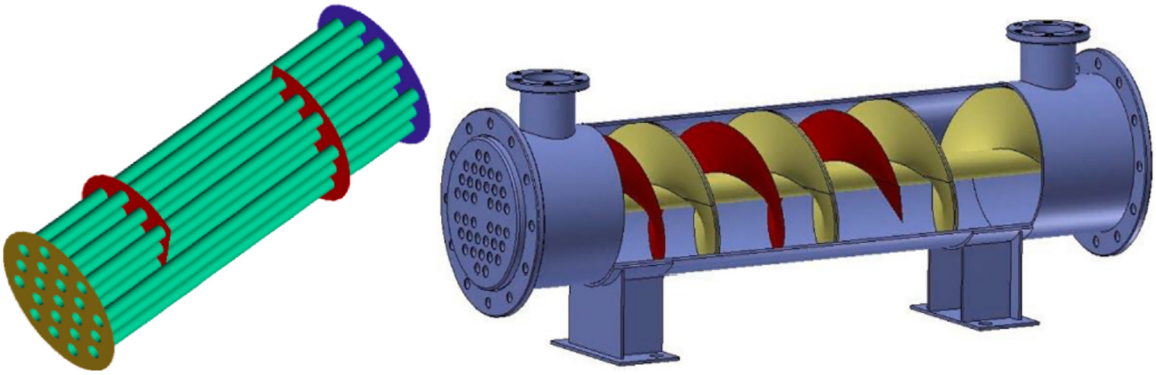

**Figure 1:** STHX with segmental baffle (Kaleru et al. 2022b).

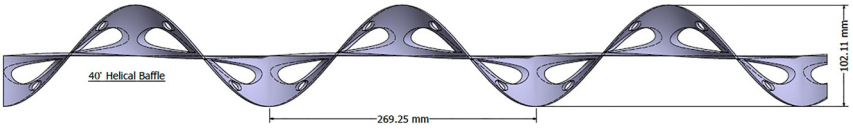


**Figure 2:** 40° helical baffle (Kaleru et al. 2022b).

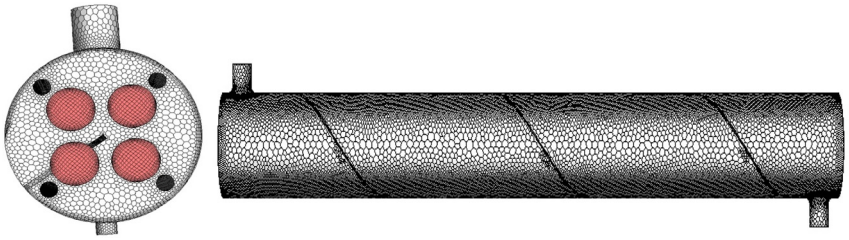

**Figure 3:** 40° helical baffle with mesh geometry (Kaleru et al. 2022b).

**Table 1:** Thermophysical properties of base fluid and nanofluids.

| Nanofluid | Volume fraction | Density in $\frac{kg}{m^3}$ | Cp in $\frac{J}{kg\,K}$ | Thermal conductivity in $\frac{W}{m\,K}$ | Dynamic viscosity in Pa s |
|---|---|---|---|---|---|
| Hot fluid (hot water) | | 1004.91450 | 4161.971514 | 0.645992912 | 0.000335160 |
| Base fluid (cold water) | | 1001.15859 | 4150.148415 | 0.614843598 | 0.000706773 |
| $Al_2O_3$ | 0.01% | 1027.147008 | 4004.7268 | 0.63254 | 0.0007248 |
| | 0.03% | 1079.123836 | 3734.8967 | 0.66898 | 0.0007627 |
| | 0.05% | 1131.100665 | 3489.8653 | 0.70687 | 0.0008035 |
| Cu | 0.01% | 1080.547008 | 3806.8650 | 0.63339 | 0.0007248 |
| | 0.03% | 1239.323836 | 3252.2381 | 0.67162 | 0.0007627 |
| | 0.05% | 1398.100665 | 2823.5849 | 0.71145 | 0.0008035 |

Blasius equation is (Kanti et al. 2021a; Mohammadiun et al. 2016)

$$f_t = \frac{0.316}{\mathrm{Re}_t^{0.25}} \tag{3}$$

Darcy friction factor is (Moradi et al. 2019)

$$f_t = \frac{1}{\left(1.82\log\left(\mathrm{Re}_t\right) - 1.64\right)^2} \tag{4}$$

Reynolds number of tube fluid (Kaleru et al. 2022a):

$$\mathrm{Re}_t = \frac{\rho \vartheta_t d_i}{\mu_t} \tag{5}$$

Prandtl number for base fluid (Kanti et al. 2021a; Kaleru et al. 2022a):

$$\mathrm{Pr}_t = \frac{\left(\mu C_p\right)_t}{k_t} \tag{6}$$

The Density of nanofluid is computed from mixture theory (Ahmed et al. 2021b; Gugulothu and Sanke 2022b)

$$\rho_{nf} = \varphi\rho_{np} + \rho_{bf}(1-\varphi) \tag{7}$$

Specific heat of nanofluid is (Gugulothu and Sanke 2022a)

$$(\rho C_p)_{nf} = \varphi(\rho C_p)_{np} + (1-\varphi)(\rho C_p)_{bf} \tag{8}$$

Maxwell model (Gugulothu and Sanke 2022b)

$$k_{nf} = k_{bf}\frac{k_{np} + (m-1)k_{bf} + (m-1)\varphi(k_{np} - k_{bf})}{k_{np} + (m-1)k_{bf} - \varphi(k_{np} - k_{bf})} \tag{9}$$

According to literature Timofeeva et al. (2007) listed that spherical particles are better to enhance the greater thermal conductivity. So, for same particles empirical shape factor i.e. $m = 3$ taken by pioneer's in their research works (Gugulothu and Sanke, 2022b; Keblinski et al. 2002; Vajjha and Das 2009).

Brinkman equation (Gugulothu and Sanke, 2022b; Kaleru et al. 2022a)

$$\mu_{nf} = \frac{\mu_{bf}}{(1-\varphi)^{2.5}} \tag{10}$$

Nusselt number is (Gugulothu and Sanke 2022a; Gugulothu and Sanke 2022b)

$$\mathrm{Nu}_t = \frac{h_t d_i}{k_{bf}} \tag{11}$$

Nusselt number for Dittus–Boelter equation is (Kanti et al. 2021a; Kaleru et al. 2022a)

$$\mathrm{Nu}_c = 0.023\mathrm{Re}_c^{0.8}\mathrm{Pr}_c^{0.4} \tag{12}$$

Nusselt number for Promvonge and Skullong (2019)

$$\mathrm{Nu}_c = 0.0327\mathrm{Re}_c^{0.755}\mathrm{Pr}_c^{0.4} \tag{13}$$

Thermal Performance Enhancement Factor (Dalkilic et al. 2020; Kaleru et al. 2022b; Mustafa et al. 2022):

$$\mathrm{TEF} = \frac{\left(\frac{\mathrm{Nu}_{\mathrm{improved}}}{\mathrm{Nu}_{\mathrm{base}}}\right)}{\left(\frac{f_{\mathrm{improved}}}{f_{\mathrm{base}}}\right)^{\frac{1}{3}}} \tag{14}$$

Table 1 depicts the physical properties of cold, hot fluid, and nanofluids of $Al_2O_3$, and Cu. The physical properties of cold and hot fluids are computed utilizing literature Gugulothu and Sanke (2022a), Gugulothu and Sanke (2022b), and Kaleru et al. (2022a) those are listed in Equations (7)–(10).

## 5 Validation

Gugulothu and Sanke (2022a) validated this by comparing the shell side friction factor, tube side Nusselt number and friction factor, and Overall HTC with the literature that explores the work of Chen et al. (2015). After that Gugulothu and Sanke (2022b) validated using numerical calculation of Nusselt number, and friction factor with Chen et al. (2015) experimental work and found good agreement. For further validation done by Kaleru et al. (2022a) using tube side Nusselt number of literature models like Dittus–Boelter (12), Syam Sundar et al., Notter Rouse, and Gnielinski equation and found favorable agreement in their studies. In this research paper, the friction factor data of water is validated with tube side friction factor of Blasius equation and Darcy friction factor (4) and noticed good agreement in trend follows and deviation is 2.77–2.80% for Darcy friction factor (4), 0.35–1.02% for present geometry which is shown in Figure 4.

Figure 5 gives the variation of tube side Nusselt number with shell side mass flow rate, in comparison with the Promvonge and Skullong (2019) Equation (13), Dittus–Boelter Equation (12), and pressure study of a plain tube. From Figure 5 it is clear that this study is a favorable agreement with the Dittus–Boelter Equation (12), and the Promvonge and Skullong (2019) Equation (13). The maximum enhancement of the Nusselt number is 3% when compared with the Promvonge and Skullong (2019) Equation (13), and closed with the Dittus–Boelter Equation (12).

## 6 Results and discussions

Figure 6 shows the tube side Nusselt number of $Al_2O_3$ nanofluid by varying shell side mass flow rate. In Figure 6, the Nusselt number is premeditated using Equation (11). In Figure 6, the Nusselt number increases with the increase of

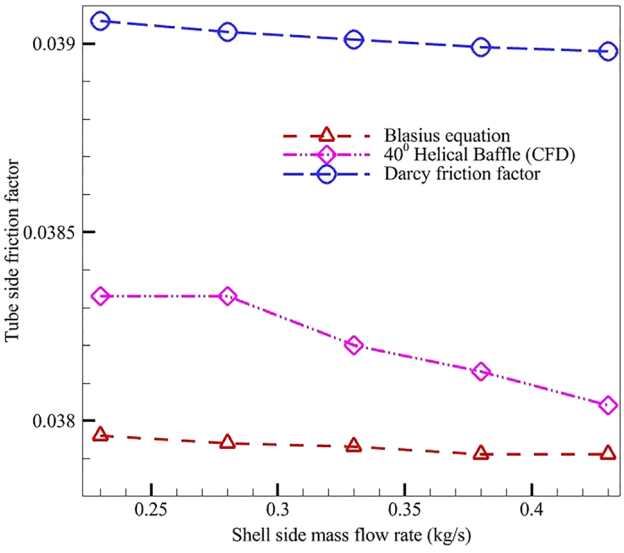


**Figure 4:** Tube side friction factor.

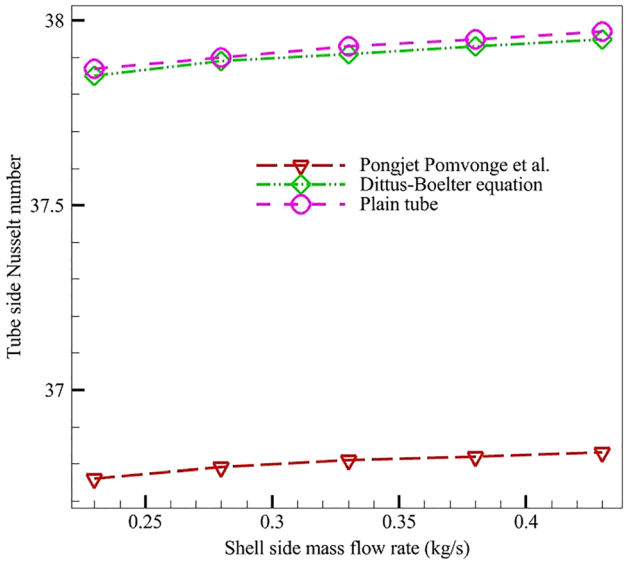


**Figure 5:** Tube side Nusselt number.

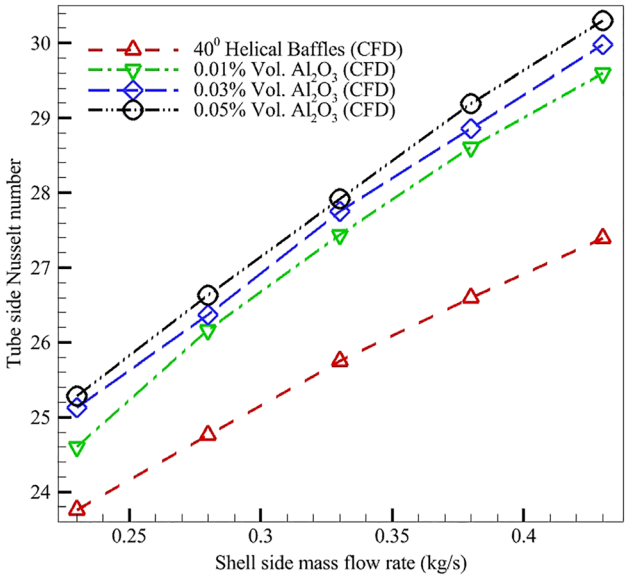


**Figure 6:** Tube side Nusselt number with $Al_2O_3$ nanofluid.

shell side mass flow rate as well as the volume fraction of nanofluids. Higher the Nusselt number for higher mass flow rate and higher volume fraction. The Nusselt number enhancement is 3.45–7.47%, 5.45–8.64%, and 6.01–9.60% for 0.01, 0.03, and 0.05% volume concentration of $Al_2O_3/H_2O$ nanofluid respectively when compared with base fluid.

Figure 7 indicates the tube side Nusselt number with a variation of shell side mass flow rate extended from 0.23 to 0.43 kg/s along with a variation of nanofluids volume concentrations from 1 to 5%. The tube side Nuselt number is premeditated using Equation (11). The tube side Nusselt number increases with an increase of shell side mass flow rate and volume concentration of $Cu/H_2O$ nanofluid which is passing through tubes. The reason for the same is the mixing of $Cu/H_2O$ nanoparticles in a base fluid to improve thermal conductivity. The enhancement of Nusselt number is 0.86–1.44%, 1.72–2.21%, and 2.42–3.18% for 0.01, 0.03, and 0.05% volume concentration of Cu nanofluid respectively although examine to the base fluid.

In Figure 8 tube side Nusselt number of $Al_2O_3/H_2O$ and $Cu/H_2O$ in terms of shell side mass flow rate is investigated. In Figure 8 values of the tube side, the Nusselt number is premeditated utilizing Equation (11). By increasing the shell side mass flow rate, the tube side Nusselt number increases and showing that higher mass flow rates give a higher tube side Nusselt number. Due to lower density, $Al_2O_3/H_2O$ nanofluids travel with more velocity. The Nusselt number enhancement is 3.68–6.63% at 0.05% volume concentration of $Al_2O_3/H_2O$ nanofluid although examine to 0.05% volume concentration of $Cu/H_2O$ nanofluid.

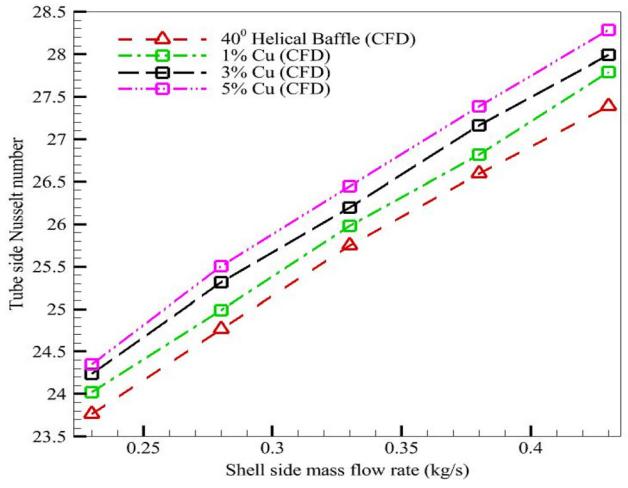


**Figure 7:** Tube side Nusselt number with Cu nanofluid.

Figure 9 depicts the tube side friction factor with the shell side mass flow rate as well as volume concentrations of $Al_2O_3$ nanofluid. Figure 9 is calculated using Equation (2), which follows the decreasing trend by increasing the shell side fluid flow rate and increases with the increase of volume concentrations of $Al_2O_3$ nanofluid. The maximum penalty in tube side friction factor is 3.23%, 15.54%, and 14.76% for 0.01, 0.03, and 0.05% volume concentrations of $Al_2O_3/H_2O$ nanofluid respectively.

In Figure 10 the tube side friction factor is compared with base fluid and $Cu/H_2O$ nanofluid at different volume concentrations ranging from 0.01 to 0.05%. In Figure 10 the tube side friction factor enhances with the enhancement of

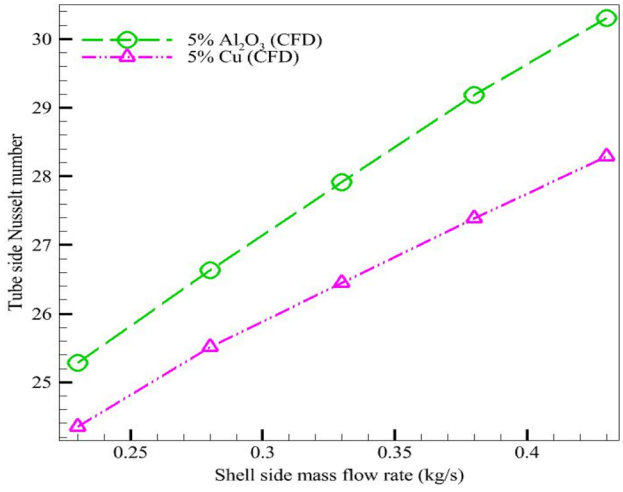


**Figure 8:** Tube side Nusselt number with $Al_2O_3$ and Cu nanofluids.

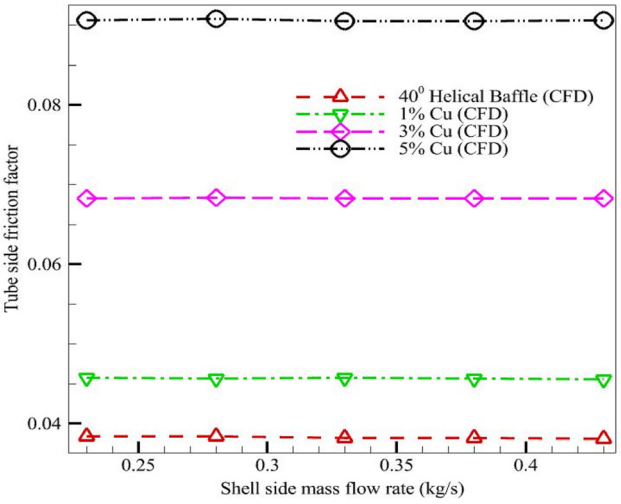


**Figure 10:** Tube side friction with Cu nanofluid.

Cu/$H_2O$ nanofluid volume concentrations and slightly decreases with the increased shell side mass flow rate. The maximum penalty in friction factor is 16.56%, 44.26%, and 58.00% for 0.01, 0.03, and 0.05% volume concentrations of Cu/$H_2O$ nanofluid.

Figure 11 shows the friction factor along with the mass flow rate of shell fluid and 5% volume concentrations of $Al_2O_3$, and Cu/$H_2O$ nanofluids. In Figure 11, the friction factor of 0.05% nanofluid is computed by utilizing Equation (2). The friction factor slightly decreases with the enhancement of the shell side mass flow rate ranging from 0.23 to 0.43 kg/s. In Figure 10, 0.05% Cu/$H_2O$ nanofluid shows a higher friction factor when compared to 0.05% $Al_2O_3$ nanofluid. The maximum penalty in friction factor is 39.86% with Cu/$H_2O$ nanofluid when compared with $Al_2O_3$/$H_2O$ nanofluid at 5% volume concentrations.

Figure 12 shows the Thermal Performance Enhancement Factor (TEF) of $Al_2O_3$ nanofluids at different volume concentrations by diverse shell side mass flow rates. This TEF value is calculated using Equation (14). The TEF values are increasing with the increase of shell side mass flow rate in addition to the volume concentration of $Al_2O_3$/water nanofluids. From Figure 12, it is clear that the higher TEF values at higher shell side mass flow rates, and higher volume concentrations. The justification for this is the addition of nanoparticles in the base fluid.

Figure 13 shows the thermal performance enhancement factor for 0.01, 0.03, and 0.05% volume concentrations of Cu/$H_2O$ nanofluid. This TEF value is calculated using Equation (14). From Figure 13, the maximum enhancement in TEF is 12.50% for a 0.05% volume concentration of Cu/$H_2O$

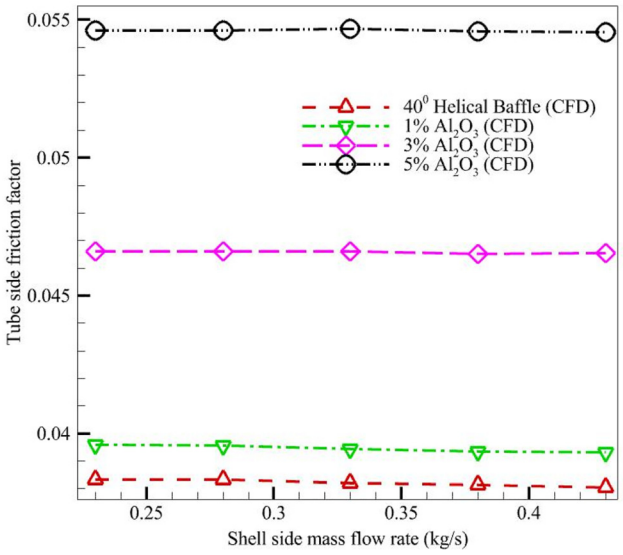


**Figure 9:** Tube side friction with $Al_2O_3$ nanofluid.

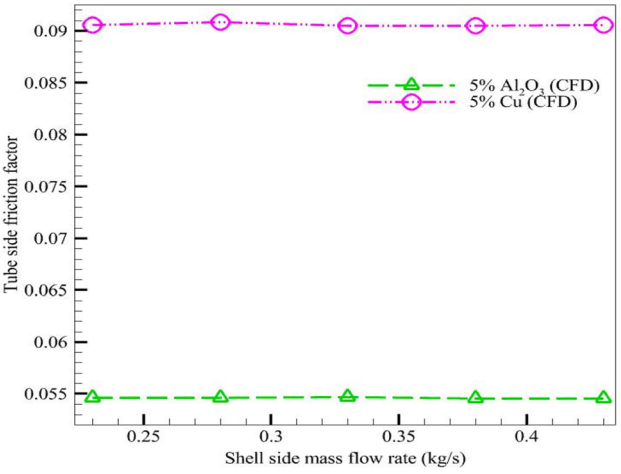


**Figure 11:** Tube side friction with $Al_2O_3$ and Cu nanofluid.

nanofluid at a higher shell side mass flow rate when compared to a 0.01% volume concentration of $Cu/H_2O$ nanofluid. According to Nohooji et al. (2020), this nanofluid is not suggestible/acceptable for research.

Figure 14 shows the comparison plot of TEF values among the $Al_2O_3$, and Cu nanofluids at 0.05% volume concentrations with shell-side mass flow rates fluctuating from 0.23 to 0.43 kg/s. The TEF values are computed using Equation (14). In Figure 14, TEF values for $Al_2O_3/H_2O$ are more than unity and $Cu/H_2O$ is less than unity. The thermal performance enhancement factor takes account of two competing factors as Nusselt number and the friction factor was used. The enhancements in Nusselt number, due to the improvement of thermo physical properties of $Al_2O_3/H_2O$ is the main reason for it. The maximum value of TEF is achieved at a higher shell side mass flow rate and the value is 1.07 for 0.05% $Al_2O_3/H_2O$ nanofluid. Figures 11–13 obey the trends of literature Liang et al. (2019) and Liang et al. (2018).

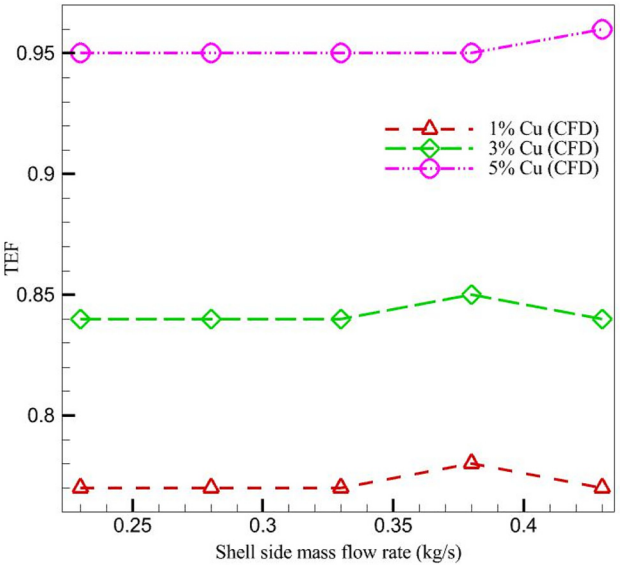


**Figure 13:** Thermal performance enhancement factor of Cu nanofluid.

## 7 Conclusions

A numerical analysis is conducted to estimate the effect of $Al_2O_3$ and Cu nanofluids on the HT rate, friction factor, and thermal performance factor of 40° helical baffles STHX. Shell side (hot water) mass flow rate varied from 0.23 to 0.43 kg/s. Water-based nanofluids are used inside the tubes with 0.01, 0.03, and 0.05% volume concentrations of $Al_2O_3$ and Cu nanofluids. Nusselt number acquired from the present investigation is compared with the Dittus–Bolter equation and Pongjet Pomvonge et al. and established to be in good

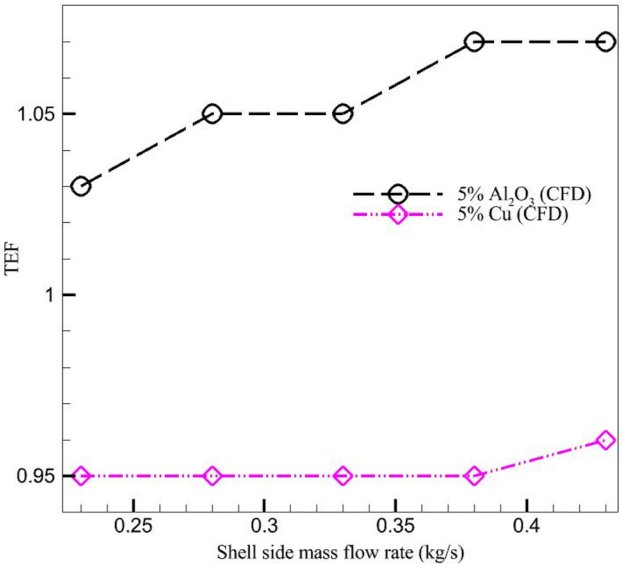


**Figure 14:** Thermal performance enhancement factor.

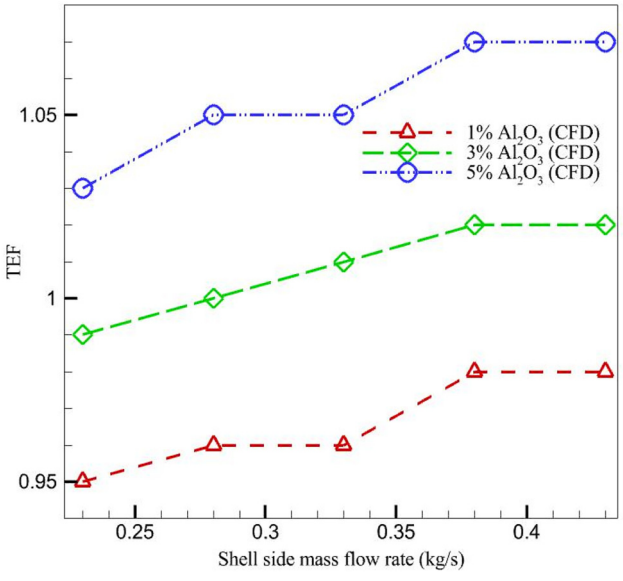


**Figure 12:** Thermal performance enhancement factor $Al_2O_3$ nanofluid.

agreement with a maximum deviation of 3%. The friction factor acquired from this study is compared with existing correlations in the literature and the maximum deviation is found to be within reasonable limits (2.88%).

The Nusselt number of the dispersed nanofluids increased with the increase of nanofluids volume concentrations and shell side mass flow rate. The maximum Nusselt number is 7.47%, 8.64%, and 9.60% for 0.01%, 0.03%, and 0.05% volume concentration of $Al_2O_3$, and 1.44%, 2.21%, and 3.18% for 0.01, 0.03, and 0.05% volume concentration of Cu nanofluids respectively. In this study, maximum enhancement in Nusselt

number is 7.50%, 8.65%, and 9.61% for $Al_2O_3$, and 1.46%, 2.23%, and 3.18% for Cu nanofluid respectively at 1, 3, and 5% volume concentrations were compared to base fluid as water. The maximum friction factor penalty is 3.23%, 15.54%, and 14.76% for 0.01%, 0.03%, and 0.05% of $Al_2O_3$, and 16.56%, 44.26%, and 58.00% for 0.01%, 0.03%, and 0.05% Cu nanofluids respectively. Friction factor is highest by 58.00% at 5% volume concentration of Cu/$H_2O$ nanofluid when compared to 40° helical baffles plain tube. Thermal Enhancement factor achieved is highest for $Al_2O_3$/$H_2O$ nanofluid.

## Nomenclature

| | |
|---|---|
| HE | heat exchanger |
| STHX | shell and tube heat exchangers |
| HTC | heat transfer coefficient |
| HT | heat transfer |
| HB | helical baffles |
| vol. | volume |

**Author contributions:** All the authors have accepted responsibility for the entire content of this submitted manuscript and approved submission.
**Research funding:** None declared.
**Conflict of interest statement:** The authors declare no conflicts of interest regarding this article.

## References

Ahmed, F., M. A. Abir, P. K. Bhowmik, V. Deshpande, and A. S. Mollah. 2021a. "Thermohydraulic Performance of Water Mixed $Al_2O_3$, $TiO_2$, and Graphene Oxide Nanoparticles for Nuclear Fuel Triangular Subchannel." *Thermal Science and Engineering Progress* 24: 100929.

Ahmed, F., M. Fuad, F. Akter, R. Gugulothu, R. K. Jilugu, S. B. Alam, and D. Kumar. 2021b. "Investigation of Entropy and Turbulence Characteristics of Water Based $Al_2O_3$, $TiO_2$, and Graphene Oxide Nanoparticles in a Triangular Rod Array." *Materials Today Proceedings*. 47 (Part 11): 3364–9.

Ahmed, F., M. M. Sumon, M. Fuad, R. Gugulothu, and A. S. Mollah. 2021c. "Numerical Simulation of Heat Exchanger for Analyzing the Performance of Parallel and Counter Flow." *WSEAS Transactions on Heat and Mass Transfer* 16: 145–52.

Ahmed, F., A. Khanam, Samylingam, N. Aslfattahi, and R. Saidur. 2022. "Assessment of Thermo-Hydraulic Performance of MXene Based Nanofluid as Coolant in a Dimpled Channel: A Numerical Approach." *Journal of Thermal Analysis and Calorimetry*. 47 (Part 11): 3364–9.

Chen, Y. P., W. H. Wan, J. F. Wu, and C. Dong. 2015. "Experimental Investigation on Performances of Trisection Helical Baffled Heat Exchangers for Oil/Water–Water Heat Transfer." *Energy Conversion and Management* 101: 460–9.

Dalkilic, A. S., B. Uluc, M. S. Cellek, A. Celen, C. Jumpholkul, K. S. Newaz, and S. Wongwises. 2020. "Single Phase Flow Heat Transfer Characteristics of Quad Channel Twisted Tape Inserts in Tubes." *International Communications in Heat and Mass Transfer* 118: 104835.

Fares, M., M. Al-Mayyahi, and M. Al-Saad. 2020. "Heat Transfer Analysis of a Shell and Tube Heat Exchanger Operated with Graphene Nanofluids." *Case Studies in Thermal Engineering* 18: 100584.

Gugulothu, R., D. N. S. Somanchi, P. Kaluri, and N. Deepika. 2017a. "Solar Water Distillation Using Different Phase Change Materials." *Materials Today Proceedings* 4 (2): 314–21.

Gugulothu, R., N. S. Somanchi, K. Vijaya Kumar Reddy, and K. Akkiraju. 2017b. "A Review on Enhancement of Heat Transfer in Heat Exchanger with Different Inserts." *Materials Today Proceedings* 4: 1045–50.

Gugulothu, R., K. V. K. Reddy, N. S. Somanchi, and E. L. Adithya. 2017c. "A Review on Enhancement of Heat Trasnfer Techniques." *Materials Today Proceesings* 4: 1051–6.

Gugulothu, R., N. S. Somanchi, K. V. K. Reddy, and K. Akkiraju. 2017d. "A Review on Enhancement of Heat Transfer in Heat Exchanger with Different Inserts." *Materials Today Proceedings* 4: 1045–50.

Gugulothu, R., N. Sanke, and A. V. S. S. K. S. Gupta. 2019. "Numerical Study of Heat Transfer Characteristics in Shell and Tube Heat Exchanger." In *Numerical Heat Transfer and Fluid Flow, Lecture Notes in Mechanical Engineering*, 375–83.

Gugulothu, R., N. Sanke, F. Ahmed, and R. K. Jilugu. 2021. "Numerical Study on Shell and Tube Heat Exchanger with Segmental Baffle." In Bansal, J. C., K. Deep, A. K., Nagar (Series Eds.), *Proceedings of International Joint Conference on Advances in Computational Intelligence, Algorithms for Intelligent Systems, IJCACI* 2020. 309–18. Springer Nature Singapore Pte Ltd.

Gugulothu, R., N. Sanke, F. Ahmed, N. S. Somanchi, and M. T. Naik. 2022a. "Numerical Investigation of Baffle Spacing in a Shell and Tube Heat Exchanger with Segmental Baffle." In *Applied Analysis, Computation and Mathematical Modelling in Engineering, Lecture Notes in Electrical Engineering*, Vol. 897, 83–98.

Gugulothu, R., N. Sanke, S. Nagadesi, and R. K. Jilugu. 2022b. "Thermal Hydraulic Performance of Helical Baffle Shell and Tube Heat Exchanger Using RSM Method." In *Applied Analysis, Computation and Mathematical Modelling in Engineering, Lecture Notes in Electrical Engineering*, Vol. 897: 167–87.

Gupta, M., N. Arora, R. Kumar, S. Kumar, and N. Dilbaghi. 2014. "A Comprehensive Review of Experimental Investigations of Forced Convective Heat Transfer Characteristics for Various Nanofluids." *International Journal of Mechanical and Materials Engineering* 9 (11): 1–21.

Gugulothu, R., and N. Sanke. 2022a. "Use of Segmental Baffle in Shell and Tube Heat Exchanger for Nano Emulsions." *Journal of Heat Transfer*: 1–22. https://doi.org/10.1002/htj.22418.

Gugulothu, R., and N. Sanke. 2022b. "Effect of Helical Baffles and Water Based $Al_2O_3$, CuO, and $SiO_2$ Nanoparticles in the Enhancement of Thermal Performance for Shell and Tube Heat Exchanger." *Journal of Heat Transfer*: 1–26. https://doi.org/10.1002/htj.22474.

Heris, S. Z., S. H. Noie, E. Talaii, and J. Sargolzaei. 2011. "Numerical Investigation of $Al_2O_3$/Water Nanofluid Laminar Convective Heat Transfer through Triangular Ducts." *Nanosclae Research Letters* 6: 1–11.

Kaleru, A., S. Venkatesh, and N. Kumar. 2022a. "Theoretical and Numerical Study of a Shell and Tube Heat Exchanger Using 22% Cut Segmental Baffle." *Journal of Heat Transfer*. 51 (8): 1–17.

Kaleru, A., S. Venkatesh, and N. Kumar. 2022b. "Numerical and Experimental Study of a Shell and Tube Heat Exchanger for Different Baffles." *Journal of Heat Transfer*. 51 (13): 1–22.

Kanti, P., K. V. Sharma, Z. Said, and E. Bellos. 2021a. "Numerical Study on the Thermo-Hydraulic Performance Analysis of Fly Ash Nanofluid." *Journal of Thermal Analysis and Calorimetry*. https://doi.org/10.1007/s10973-020-10533-0.

Kanti, P., K. V. Sharma, Z. Said, and V. Kesti. 2021b. "Entropy Generation and Friction Factor Analysis of Fly Ash Nanofluids Flowing in a Horizontal Tube: Experimental and Numerical Study." *International Journal of Thermal Sciences* 166: 106972.

Kanti, P. K., K. V. Sharma, Z. Said, and M. Gupta. 2021c. "Experimental Investigation on Thermo-Hydraulic Performance of Water-Based Fly Ash-Cu Hybrid Nanofluid Flow in a Pipe at Various Inlet Fluid Temperatures." *International Communications in Heat and Mass Transfer* 124: 105238.

Kanti, P. K., K. V. Sharma, A. A. Minea, and V. Kesti. 2021d. "Experimental and Computational Determination of Heat Transfer, Entropy Generation and Pressure Drop under Turbulent Flow in a Tube with Fly Ash-Cu Hybrid Nanofluid." *International Journal of Thermal Sciences* 167: 107016.

Keblinski, P., S. R. Phillpot, S. U. S. Choi, and J. A. Eastman. 2002. "Mechanisms of Heat Flow in Suspensions of Nano Sized Particles (Nanofluids)." *International Journal of Heat and Mass Transfer* 45: 855–63.

Liang, Y., P. Liu, N. Zheng, F. Shan, Z. Liu, and W. Liu. 2018. "An Experimental and Numerical Study of Heat Transfer and Flow Characteristics of Laminar Flow in a Circular Tube with Wedge Shaped Wavy Tape Inserts." In *Proceedings of the ASME, 2018, International Mechanical Engineering Congress and Exposition IMECE2018*.

Liang, Y., P. Liu, N. Zheng, F. Shan, Z. Liu, and W. Liu. 2019. "Numerical Investigation of Heat Transfer and Flow Characteristics of Laminar Flow in a Tube with Centre Tapered Wavy Tape Insert." *Applied Thermal Engineering* 148: 557–67.

Maghrabie, H. M., M. Attalla, and A. A. A. Mohsen. 2021. "Performance Assessment of a Shell and Helically Coiled Tube Heat Exchanger with Variable Orientations Utilizing Different Nanofluids." *Applied Thermal Engineering* 182: 116013.

Malika, M., and S. S. Sonawane. 2021. "The Sono-Photocatalytic Performance of a Novel Water Based $Ti^{+4}$ Coated $Al(OH)_3$-MWCNT's Hybrid Nanofluid for Dye Fragmentation." *International Journal of Chemical Reactor Engineering*.

Malika, M., and S. S. Sonawane. 2022. "The Sono-Photocatalytic Performance of a $Fe_2O_3$ Coated $TiO_2$ Based Hybrid Nanofluid under Visible Light via RSM." *Colloids and Surfaces A: Physicochemical and Engineering Aspects* 641: 128545.

Malika, M., R. Bhad, and S. S. Sonawane. 2021. "ANSYS Simulation Study of a Low Volume Fraction CuO–ZnO/water Hybrid Nanofluid in a Shell and Tube Heat Exchanger." *Journal of the Indian Chemical Society* 98: 100200.

Mashayekhi, R., E. Khodabandeh, M. Bahiraei, L. Bahrami, D. Toghraie, and O. Ali Akbari. 2017. "Application of a Novel Conical Strip Insert to Improve the Efficacy of Water-Ag Nanofluid for Utilization in Thermal Systems: A Two-phase Simulation." *Energy Conversion and Management* 151: 573–86.

Mohammadiun, H., M. Mohammadiun, M. Hazbehian, and H. Maddah. 2016. "Experimental Study of Ethylene Glycol Based $Al_2O_3$ Nanofluid Turbulent Heat Transfer Enhancement in the Corrugated Tube with Twisted tapes." *Heat and Mass Transfer* 52: 141–51.

Moradi, A., D. Toghraie, A. H. M. Isfahani, and A. Hosseinian. 2019. "An Experimental Study on MWCNT-Water Nanofluids Flow and Heat Transfer in Double Pipe Heat Exchanger Using Porous Media." *Journal of Thermal Analaysis and Calorimentry* 137: 1797–807.

Mustafa, J., S. Alqaed, M. Sharifpur, and S. Husain. 2022. "The Effect of Using Multichannel Twisted Tape and Nanofluid on the Absorber Tube's Heat Transfer and the Efficiency of a Linear Parabolic Solar Collector." *Sustainable Energy Technologies and Assessments* 52: 102329.

Niwalkar, A. F., J. M. Kshirsagar, and K. Kulkarni. 2019. "Experimental Investigation of Heat Transfer Enhancement in Shell and Helically Coiled Tube Heat Exchanger Using $SiO_2$/Water Nanofluids." *Materials Today Proceedings* 18: 947–62.

Nohooji, A. B., D. Toghraie, F. Pourfattah, O. A. Akbari, and R. Mashayekhi. 2020. "Computational Modeling of Porous Medium inside a Channel with Homogeneous Nanofluid." *Journal of Thermal Analysis and Calorimetry* 140: 843–58.

Pak, B. C., and Y. I. Cho. 2007. "Hydrodynamic and Heat Transfer Study of Dispersed Fluids with Submicron Metallic Oxide Particles." *Experimental Heat Transfer: A Journal of Thermal Energy Generation, Transport, Storage, and Conversion* 11 (2): 151–70.

Promvonge, P., and S. Skullong. 2019. "Heat Transfer in Solar Receiver Heat Exchanger with Combined Punched V-Ribs and Chamfer V-Grooves." *International Journal of Heat and Mass Transfer* 143: 118486.

Reddy, V. K., N. S. Somanchi, R. S. R. Devi, R. Gugulothu, and B. S. P. Kumar. 2015. "Heat Transfer Enhancement in a Double Pipe Heat Exchanger Using Nanofluids." In *Proceedings of the 17th ISME Conference, 3rd–4th October, 2015, Organized by IIT Delhi*.

Reddy, K. V. K., B. S. P. Kumar, R. Gugulothu, K. Anuja, and P. V. Rao. 2017. "CFD Analysis of a Helically Coiled Tube in Tube Heat Exchanger." *Materials Today Proceedings* 4: 2341–9.

Somanchi, N. S., B. A. Prasad, R. Gugulothu, R. K. Nagula, and K. S. P. Dinesh. 2015a. "Performance of Solar Still with Different Phase Change Materials." *International Journal of Energy and Power Engineering* 4: 33–7.

Somanchi, N. S., R. S. R. Devi, R. Gugulothu, and S. P. K. Bellam. 2015b. "Experimental Investigations on Turbulent Flow Heat Transfer Enhancement in a Horizontal Tube Using Inserts." In *Proccedings of the 17th ISME Conference (ISME17), 3rd–4th October, 2015, IIT Delhi*.

Somanchi, N. S., R. Sri Rama Devi, and R. Gugulothu. 2014a. "Experimental Investigations on Heat Transfer Enhancement in a Horizontal Tube Using Converging and Diverging Conical Strip Inserts." *Applied Mechanics and Materials* 592–594: 1590–5.

Somanchi, N. S., S. R. D. Rangisetty, S. P. K. Bellam, R. Gugulothu, and S. Bellam. 2014b. "Experimental Investigations on Heat Transfer Enhancement in a Horizontal Tube Using Converging and Diverging Conical Strips." In *Proceedings of the ASME 2014 Gas Turbine India Conference, GTINDIA2014, 15th–17th December*.

Sarada, S. N., R. S. R. Devi, and R. Gugulothu. 2014. "Turbulent Flow Heat Transfer Enhancement in a Horizontal Tube Using Inserts." In *Proceedings of 1st International Conference on Mechanical Engineering: Emerging Trends for Sustainability*, 1078–85.

Said, Z., R. Saidur, A. Hepbasli, and N. A. Rahim. 2014. "New Thermophysical Properties of Water Based $TiO_2$ Nanofluid-The Hysteresis Phenomenon Revisited." *International Communications in Heat and Mass Transfer* 58: 85–95.

Shilpi, A. V., and N. Aggarwal. 2020. "Heat Transfer Model to Study Nano Fluids & It's Application." *Materials Today Proceedings*. 37 (Part 2): 3074–6.

Sundar, L. S., M. H. Farooky, S. N. Sarada, and M. K. Singh. 2013. "Experimental Thermal Conductivity of Ethylene Glycol and Water

Mixute Based Low Volume Concentration of $Al_2O_3$, and CuO Nanofluids." *International Communications in Heat and Mass Transfer* 41: 41–6.

Thakur, P., N. Kumar, and S. S. Sonawane. 2021. "Enhancement of Pool Boiling Performance Using MWCNT Based Nanofluids: A Sustainable Method for the Waste Water and Incinerator Heat Recovery." *Sustainable Energy Technologies and Assessments* 45: 101115.

Thakur, P., S. S. Sonawane, S. H. Sonawane, and B. A. Bhanvase. 2020. "Nanofluids-based Delivery System, Encapsulation of Nanoparticles for Stability to Make Stable Nanofluids." *Encapsulation of Active Molecules and their Delivery System*.

Timofeeva, E. V., A. N. Gavrilov, J. M. McCloskey, Y. V. Tolmachev, S. Sprunt, L. M. Lopatina, and J. V. Selinger. 2007. "Thermal Conductivity and Particle Agglomeration in Alumina Nanofluids: Experiment and Theory." *Physical Review E* 76: 061203.

Velagapudi, V., R. K. Konijeti, and C. S. K. Aduru. 2008. "Empirical Correlations to Predict Thermophysical and Heat Transfer Characteristics of Nanofluids." *Thermal Science* 12: 27–37.

Vajjha, R. S., and D. K. Das. 2009. "Experimental Determination of Thermal Conductivity of Three Nanofluids and Development of New Correlations." *International Journal of Heat and Mass Transfer* 52: 4675–82.

Zeinali, S., M. N. Esfahany, and G. Etemad. 2007. "Numerical Investigation of Nanofluid Laminar Convective Heat Transfer through Tube." *Numerical Heat Transfer Part A* 52: 1043–58.

Zeinali-Heris, S., A. Kazemi-Beydokhti, S. H. Noie, and S. Rezvan. 2012. "Numerical Study on Convective Heat Transfer of $Al_2O_3$/water, CuO/water and Cu/water Nanofluids through Square Cross Section Duct in Laminar Flow." *Engineering Applications of Computational Fluid Mechanics* 6 (1): 1–14.